



Ventilation increase using radiative cooling and phase change material at no additional energy cost in high ambient temperature countries

Walid Chakroun, Sorour Alotaibi, Jennifer Karam, Elvire Katramiz, Kamel Ghali & Nesreen Ghaddar

To cite this article: Walid Chakroun, Sorour Alotaibi, Jennifer Karam, Elvire Katramiz, Kamel Ghali & Nesreen Ghaddar (2022) Ventilation increase using radiative cooling and phase change material at no additional energy cost in high ambient temperature countries, Science and Technology for the Built Environment, 28:7, 807-822, DOI: [10.1080/23744731.2022.2045134](https://doi.org/10.1080/23744731.2022.2045134)

To link to this article: <https://doi.org/10.1080/23744731.2022.2045134>



Published online: 11 Mar 2022.



Submit your article to this journal [↗](#)



Article views: 335



View related articles [↗](#)



View Crossmark data [↗](#)



Citing articles: 3 View citing articles [↗](#)



Ventilation increase using radiative cooling and phase change material at no additional energy cost in high ambient temperature countries

WALID CHAKROUN^{1*}, SOROUR ALOTAIBI¹, JENNIFER KARAM², ELVIRE KATRAMIZ², KAMEL GHALI² and NESREEN GHADDAR²

¹Mechanical Engineering Department, Kuwait University, Kuwait City, Kuwait

²Mechanical Engineering Department, American University of Beirut, Beirut, Lebanon

In this work, a passive system composed of a radiative cooling (RC) panel combined with two phase change material (PCM) storage tanks was integrated with a conventional air conditioning (AC) system to minimize energy consumption of cooling the high temperature fresh air in the hot climate like Kuwait. The cooling power produced by the RC panel was used to charge the PCM storage tanks. One of these tanks was used for precooling the supplied fresh air (tank 1) and another for enhancing the coefficient of performance (COP) of the AC system by cooling the ambient air entering the condenser (tank 2). A mathematical model was developed for the proposed system and simulations were conducted for a typical Kuwaiti residence for the entire summer season extending from April to October. It was found that tank 1 resulted in an increase in the fresh air intake at zero energy expenses from 30 l/s/person to 190 l/s/person, with no required ventilation load from the AC system. Furthermore, tank 2 enhanced the COP by 10.5%. Thus, the overall energy consumption of the AC system was reduced by 22.3% with respect to the conventional AC system.

1. Introduction

During the last decades, the need for cooling in the building sector has witnessed a dramatic increase due to population growth, urbanization and climate change. This is especially true for countries in the Gulf region usually characterized by hot summers (Alotaibi 2011)(Alotaibi 2011)(Alotaibi 2011)(Alotaibi 2011)(Alotaibi 2011)(Alotaibi 2011)(Alotaibi 2011). Moreover, it is necessary to improve the indoor air quality (IAQ), given the rapid spread of the

SARS-CoV-2 virus in tight conditioned building. Increasing fresh air ventilation is a key solution as it dilutes biological indoor contaminants and reduce cross-contamination between occupants (Dai and Zhao 2020; Li et al. 2007) .

Both the residential and commercial buildings in the Gulf region rely heavily on mechanical cooling and ventilation installations (Park, Kim, and Lee 2019; Kellow 1989). However, such techniques are expensive, energy-intensive, and can further exacerbate the climate change problem by contributing to greenhouse gases emissions (Williams et al. 2012). In contrast with conventional air conditioning, passive cooling techniques – given adequate design and control of supply conditions - can provide the same cooling effect with minimal environmental impacts and allow for increases in the ventilation; improving IAQ at a reduced energy cost.

Many passive and cost-effective cooling strategies have been extensively studied in the literature. Some of these strategies rely on smart employment of the building fabric (i.e., louver shading devices, double glazed windows, insulation, reflective paints...) (Zinzi and Fasano 2009; Al Touma et al. 2016) or on the passive cooling of the supply air through water evaporation (direct, indirect evaporative cooling) (Baakeem et al. 2019, Harrouz, Ghali, and Ghaddar 2021) Another emerging technology is the use of radiative cooling, which takes places through the net emission of electromagnetic waves from hot objects to cool ones. The setup

Received June 3, 2021; Accepted February 14, 2022

Walid Chakroun, Fellow ASHRAE, is a professor in the Mechanical Engineering Department, Kuwait University, Kuwait City, Kuwait. **Soroor Alotaibi** is an associate professor in the Mechanical Engineering Department, Kuwait University, Kuwait City, Kuwait. **Jennifer Karam** is a master mechanical engineering student at American University of Beirut, and **Elvire Katramiz** is a PhD student at the American University of Beirut, **Nesreen Ghaddar**, Fellow ASHRAE, is a professor in the Mechanical Engineering, Department, American University of Beirut, Beirut, Lebanon. **Kamel Ghali** is a professor in the Mechanical Engineering Department, American University of Beirut, Beirut, Lebanon.

*Corresponding author e-mail: wchakroun@gmail.com

consists of a specialized metallic plate that emits long-wave radiation to the outer space (i.e., heat sink) for cooling purposes. Xu et al. (2022) used radiative sky cooling as a fresh air precooling system to reduce cooling energy consumption in 6 cities having different climatic conditions. The system was able to achieve average energy savings of 10%. Zhou, Miljkovic, and Cai (2021) proposed using radiative cooling to reduce the indoor temperatures and energy consumption for a typical U.S. house. They found that the system was able to achieve high electricity consumption savings (> 2200 kWh) for hot arid regions.

Radiative cooling works in the following sequence. The emitted radiation escapes through the transparency window of the atmosphere (8–13 μm) in which the radiative emission exceeds the incoming absorbed radiation from the sun. This phenomenon is outweighed by the absorbed solar and atmospheric radiation outside the transparency window. Many studies considered enhancing the conventional radiative cooling (RC) panels by using new coating materials that are spectrally selective, have a high emissivity inside the atmospheric transparency window and low absorptivity outside it. Such materials also have high solar reflectivity in order to avoid the absorption of incident solar radiation by the RC panel during daytime (Head 1962; Gentle and Smith 2010; Orel, Gunde, and Krainer 1993; Yu et al. 2019; Jeong, Tso, et al. 2018).

Despite all the efforts to increase its effectiveness, RC faces many challenges in building applications especially in hot climate countries (Hu et al. 2020). Firstly, the RC power is not enough for large building cooling demands (Ahmad, Jarimi, and Riffat 2019). Therefore, it is more likely to assist conventional air conditioning systems. Jeong, Tso, et al. (2018) suggested that the passive RC system should be integrated with a conventional air conditioning system; to precool the fresh hot air supplied to the space. They found that the proposed system was able to achieve a 35% potential saving in energy consumption. Secondly, the cooling power of RC panels varies vastly between nighttime and daytime. In the absence of shortwave radiation (nighttime), the highest cooling power of the RC panels occurs while building occupants require more cooling in the daytime (Ahmad, Jarimi, and Riffat 2019; Zhao, Aili, et al. 2019). Bao et al. (2017) theoretically showed that under dry air conditions coated panels can achieve about 17°C below ambient at night and 5°C below ambient under direct solar radiation. To alleviate this problem, many literature studies implemented storage systems with RC applications to store the RC cooling energy during nighttime and use it during peak cooling demand hours (Zhang and Niu 2012; Katramiz, Al-Jebaei, et al. 2020).

Phase change materials (PCM) used in thermal storage tanks have gained a lot of attention especially when combined with RC systems. These materials have the capability to store thermal energy at relatively constant temperatures (i.e., melting temperatures) due to their high heat capacity and thermal conductivity (Shahsavari et al. 2019). Many literature studies incorporated PCM in passive systems: (Safaei, Goshayeshi, and Chaer 2019) enhanced the productivity of a solar still for desalination applications by employing PCM. (Sarafraz et al. 2019) attached a PCM filled cooling jacket to a solar panel and reported a 20%

enhancement in its thermal performance. PCM is available for a wide melting temperature range. The proper storage temperature is an important criterion for selecting a suitable PCM for passive applications (Katramiz, Al-Jebaei, et al. 2020; Kauranen, Peippo, and Lund 1991). The PCM melting temperature should be selected to enable complete solidification during nighttime and complete melting during daytime (Stritih and Butala 2007). As the cooling power of the RC panel is low during daytime and increases throughout the night (Mihalakakou, Ferrante, and Lewis 1998), this work suggests storing this cooling power in two storage tanks at two different melting temperatures. In this case, we can harvest and store all the nighttime cooling power, and utilize this stored power during peak hours to decrease the overall energy consumption of the AC system.

The RC cooling power is stored at two different temperatures (a low and high temperature), to be used according to the cooling and ventilation needs in the building. On one hand, the low temperature PCM tank can make it possible to meet the entire ventilation load at increased fresh air intake, thereby passively enhancing the IAQ. On the other hand, the high temperature PCM tank can be used to lower the temperature of the condenser ambient air (for the vapor compression system) in order to increase its coefficient of performance (COP) during peak hours of the day.

To this end, the main goal of the study is to explore the radiative cooling system performance when combined with 2 PCM tanks at 2 different melting temperatures (low melting temperature and high melting temperature) in reducing the overall energy consumption. The main novelty and originality of this paper resides in the combination and application of the proposed system: the harvested cooling power was stored at two different temperatures and used for two the different strategies intending to decrease the overall AC system energy consumption. The stored cooling power was used to 1) cool the fresh air entering the residence for ventilation purposes and 2) enhance the COP of the AC system by cooling the air entering its condenser. The efficacy of the sustainable passive system was assessed through a case study of a typical residence in dry-hot climate of Kuwait. The study is performed for the cooling months of Kuwait extending from April until October. The system consists of a hydronic RC panel combined with two PCM storage tanks at two different melting temperatures for day and nighttime ventilation purposes as well as an enhanced mechanical system operation resulting in a decrease in the overall energy consumption. An integrated mathematical model of the proposed system is developed to investigate the advantages of the proposed system in passively increasing the amount of fresh air supplied to the space throughout the day. In addition, the model studies the enhancement in the performance of the air conditioning system during peak hours of the day by precooling the air entering the condenser of the air conditioning unit.

2. System description

A hybrid cooling system composed of a conventional vapor compression AC system and a RC-PCM system is

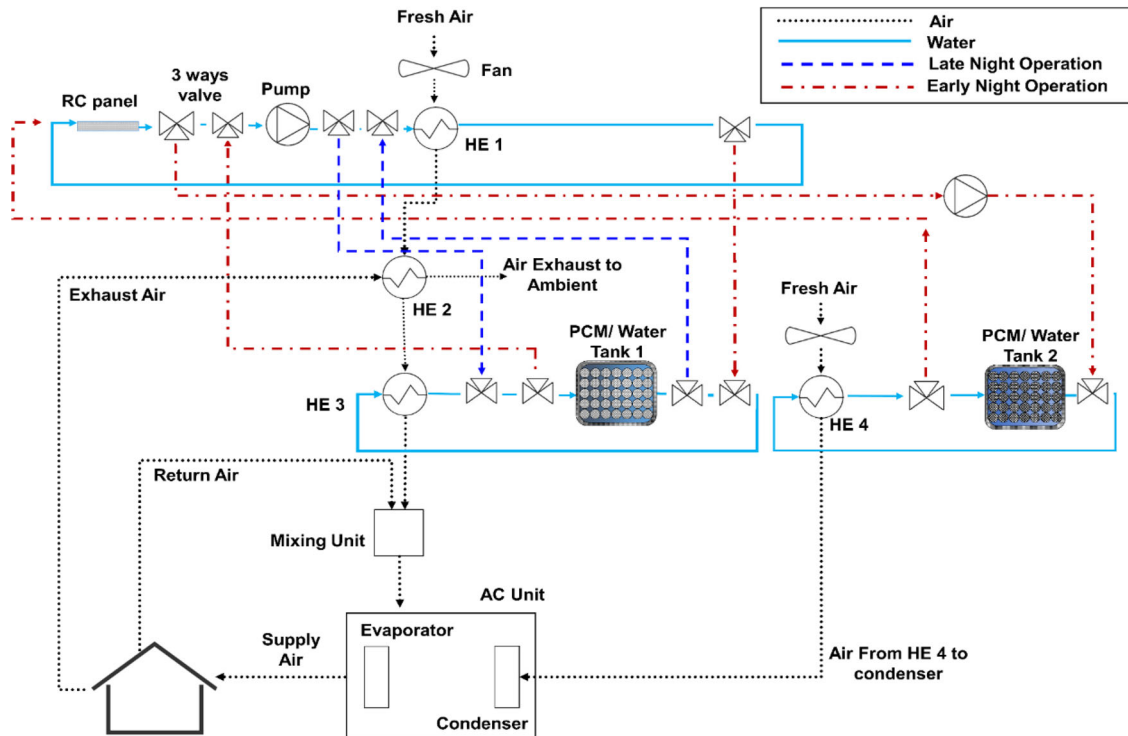


Fig. 1. Schematic of the complete hybrid system and its daytime operation.

considered in this work. The RC-PCM meets the ventilation needs of a typical Kuwaiti villa, and reduces the AC system’s energy consumption by enhancing its performance. The RC-PCM system assists the vapor compression AC system in meeting the entire ventilation load while increasing the fresh airflow supplied ($\dot{m}_{fresh\ air}$) to the villa, at zero energy cost compared to the standalone mechanical cooling system. Furthermore, the performance of the AC system is enhanced by increasing its COP and reducing the overall required electrical load for cooling. The RC-PCM system consists of a hydronic RC panel with two PCM thermal storage tanks at two different melting temperatures:

- PCM tank 1 at low melting temperature ($Tm1$): it is used for precooling the fresh air to meet the ventilation load;
- PCM tank 2 at high melting temperature ($Tm2$): it is used to improve the efficiency of the vapor compression system by increasing its coefficient of performance (COP) during peak day hours.

The complete system is shown in Figure 1. The system operation varies between three time periods based on weather conditions: a) daytime operation (Figure 1) during the period of solar radiation, b) early night operation (Figure 2a) during the period starting at the beginning of the night (i.e. absence of solar radiation) and ending when the temperature of the water out of the RC is lower than $Tm1$, and c) late night operation (Figure 2b) during the period starting when the temperature of the water out of the RC is lower than $Tm1$ and ending when the daytime starts (i.e. solar radiation period). In each period, the PCM spheres are either solidified or melted according to their surrounding water temperature. When the

water temperature surrounding the PCM falls below their melting temperature, the PCM spheres release heat until solidification. However, when the water temperature surrounding the PCM spheres rises to above their melting temperature, the PCM absorb heat until total melting. Each mode of operation is described in detail in this section.

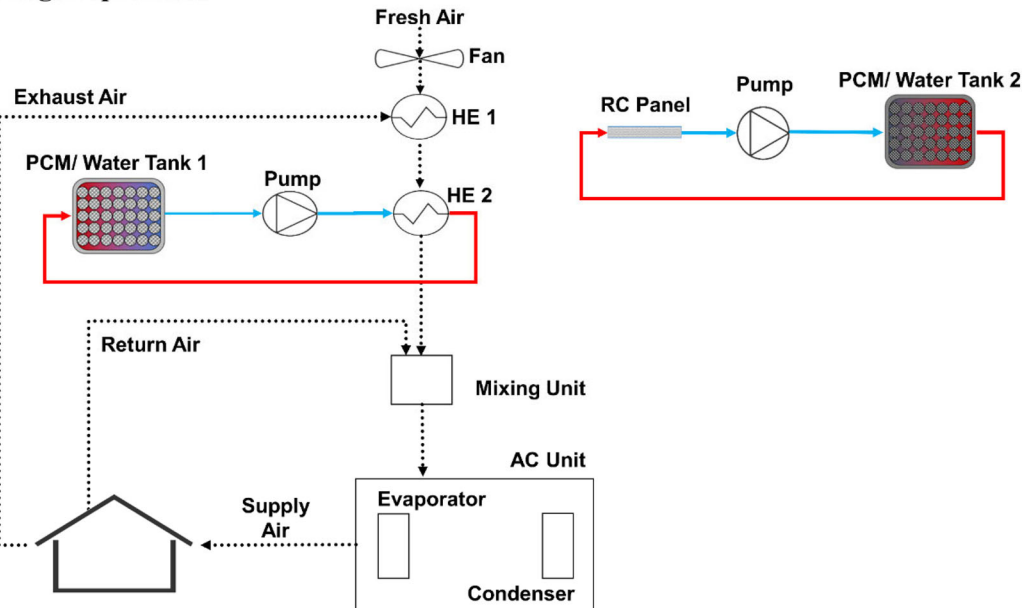
2.1. Daytime system operation

During daytime (Figure 1), the fresh air is cooled via an air-water heat exchanger (HE 1) with the cold water exiting the RC panel. The water leaving, HE 1 is circulated back to the RC panel to be cooled again in a closed loop. The cooled fresh air flows then to a second heat exchanger (HE 2) where it releases its heat to the exhaust air leaving the space. This is referred to as the “heat recovery” stage. The cooled air then flows into a third heat exchanger (HE 3) for cooling via heat exchange with the water exiting PCM tank 1. The exhaust water is circulated back to tank 1 in a closed loop where it loses its heat to the PCM. The exhaust air enters the mixing unit where it is mixed with the return air for further cooling in the AC system to meet the space cooling load. As for the cold energy stored in PCM tank 2, it is used to precool the air entering the condenser of the AC system to enhance its COP at peak hours, when the outdoor air temperature is higher than the PCM tank 2 melting temperature ($Tm2$) and the COP is at its lowest.

2.2. Early night system operation

During early hours of the night (Figure 2a), the temperature of the water exiting the RC panel is higher than the melting

a) Early night operation



b) Late night operation

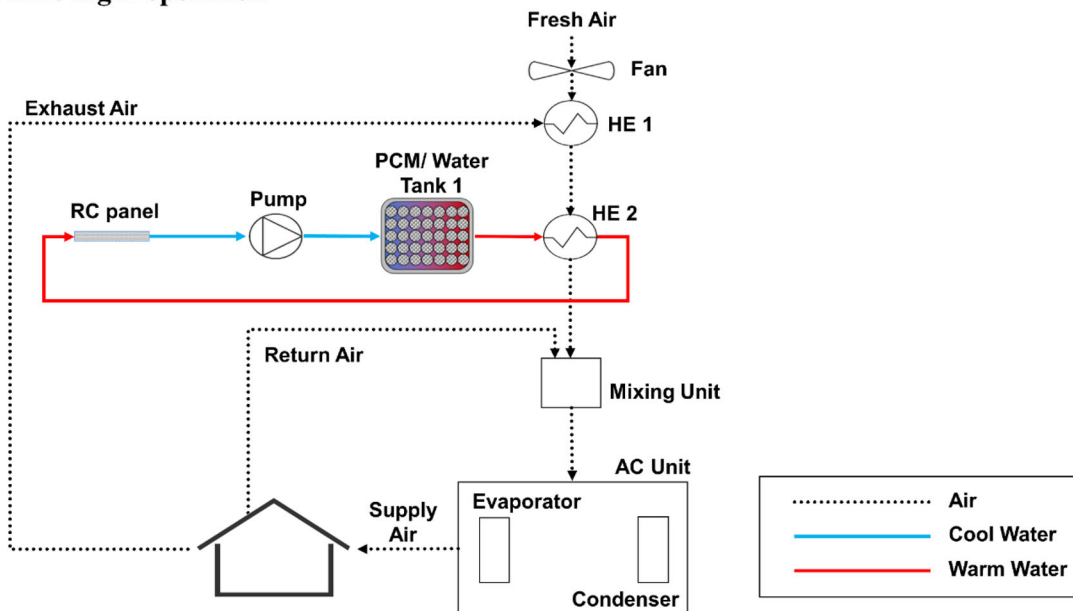


Fig. 2. Schematic of: (a) Early night operation of the system and (b) late night operation of the system.

temperature of PCM tank 1 (T_{m1}). During these hours, the early night operation is on and the cooling power of the RC panel is used to solidify PCM tank 2. At the same time, the fresh air is being cooled by heat recovery process via an air-air heat exchanger (HE 1) with the exhaust air. The fresh air then flows into a second heat exchanger (HE 2) where it is further cooled by the water exiting PCM tank 1. The water is circulated back to tank 1 in a closed loop where it loses its heat to the PCM. The cooled fresh air leaving HE 2 enters a mixing unit where it is mixed with the return air from the space. The product air is then supplied to the AC unit for further cooling.

2.3. Late night system operation

During late hours of the night (Figure 2b), when the cooling power of the RC panel increases, the water temperature leaving the hydronic panel reaches levels below T_{m1} . Thus, this cooling power is harvested in solidifying PCM tank 1. PCM tank 2 would be completely solidified by this time due to its proper sizing. The cold-water out of the RC panels flows to PCM tank 1 where the low temperature cold energy is stored at T_{m1} . The fresh air that is first cooled by heat recovery process in HE 1, then enters an air-water heat exchanger (HE 2) where it is further cooled by the water out of PCM

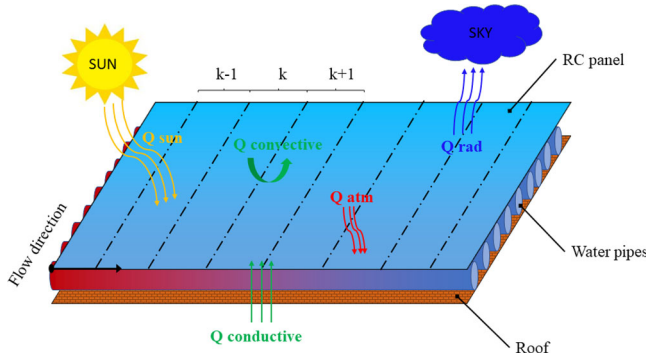


Fig. 3. Schematic of the RC panel discretized into segments and different heat transfer processes.

tank 1. The water then returns into the RC panel, whereas the fresh air undergoes the mixing process with the return air. Afterwards, air is supplied to the AC unit to meet the required cooling load of the space.

The aim of the proposed system is to increase $\dot{m}_{fresh\ air}$ supplied to the space, by harvesting the cooling power of PCM tank 1. Note that the amount of increase depends on many factors such as the size of the PCM storage tank and RC panel, as well as the outdoor conditions. The obtained increase in fresh air helps in improving the air quality indoors without any additional energy consumption. Furthermore, using PCM tank 2, the COP of the AC is enhanced by the pre-cooling of the air entering the condenser. This is expected to reduce the total energy consumption of the system with respect to the conventional AC providing the same indoor air quality (i.e. same amount of fresh air $\dot{m}_{fresh\ air}$).

3. Mathematical modelling

In this section, simplified energy balance equations were derived around each finite volume of each component of the proposed system: the hydronic RC panel and the two PCM storage tanks using the finite volume numerical approach (Dutil et al. 2011, Oguntala, Sobamowo, and Abd-Alhameed 2019). These models were adopted from Katramiz et al. (Katramiz, Al-Jebaei, et al. 2020) and integrated to simulate the operation of the system and predict the ability of the proposed system in reducing the energy consumption of the AC system.

3.1. Hydronic radiative cooling panel

The RC panel model was used to predict the water temperature through the pipes of the RC panel (Figure 3). It assumes a unidirectional variation of the water temperature through the pipes of the RC. Consequently, the panel is discretized into different segments along its length as shown in Figure 3, each having the same area A_k (m^2), and is characterized by a uniform surface temperature and a constant water temperature $T_{w,RC}$ (K). The number of segments N was chosen by running many simulations on different chosen number of segments to finally arrive to an output water temperature

independent of N , with a minimum possible computational time. In conclusion, $N=150$ was adopted. Equation (1) presents the energy balance on a segment k :

$$\begin{aligned} \rho_w V_k C_{p,w} \frac{dT_{w,RC}(t,k)}{dt} \\ = \dot{V}_{w,RC} \rho_w C_{p,w} (T_{w,RC}(t,k-1) - T_{w,RC}(t,k)) \\ - Q_{net} A_k \end{aligned} \quad (1)$$

The left term of Equation (1) represents the transient storage term. The first term to the right is the net convective heat flow and the last term is the time dependent net cooling power term. V_k (m^3) is the volume of water in segment k . ρ_w (kg/m^3) and $C_{p,w}$ ($J/kg.K$) are the density and the specific heat capacity of the water, respectively. $T_{w,RC}(t,k-1)$ (K) and $T_{w,RC}(t,k)$ (K) are respectively the inlet and outlet water temperature of segment k at time t . $\dot{V}_{w,RC}$ (m^3/s) is the volumetric flow rate of water through the pipes embedded in the RC panel. $Q_{net}(t,k)$ (W/m^2) is the time dependent net cooling power per unit area of segment k of the RC; it depends on several heat transfer processes as shown in Figure 3, and is described by the energy balance in Equation (2):

$$Q_{net}(t,k) = Q_{rad}(t,k) - Q_{atm}(t) - Q_{sun}(t) - Q_c(t,k) \quad (2)$$

where Q_{rad} (W/m^2) is the longwave radiative power emitted by the panel surface, Q_{atm} (W/m^2) is the absorbed incident atmospheric radiation, Q_{sun} (W/m^2) is the absorbed incident solar radiation, and Q_c (W/m^2) is the power lost/gained by the RC panel due to heat exchange via convection with the ambient air as well as conduction through the insulated roof ($Q_{conductive} + Q_{convective}$). The heat transfer via conduction through the roof is negligible since the roof is considered insulated and does not thereby affect the RC panel performance. As for the convective heat transfer, it is affected by the ambient conditions (mainly: wind speed and ambient temperature) and induces losses that reduce the cooling power of the RC. These losses usually range between (2% and 20%) of the total RC cooling power (Meir et al. 2002). Note that aforementioned heat transfer mechanisms were taken into consideration in the model to evaluate the cooling power of the RC panel.

3.2. PCM tanks model

The proposed storage system consists of two PCM storage tanks having two different melting temperatures. During the night, the PCM stores the cold energy from the water and solidifies, and this energy is released into the hot water during daytime (see Figure 4). Each tank is modeled as a fully insulated horizontal tank filled with spherical capsules containing PCM. The thermal model describing the behavior of this component is based on the following assumptions: (1) The width of each tank is negligible compared to its length; (2) the temperature of the water flowing through the tank varies only in one direction: longitudinally along the flow direction; (3) the heat transfer in the volume of the sphere is neglected; (4) the temperature gradient of the PCM in the

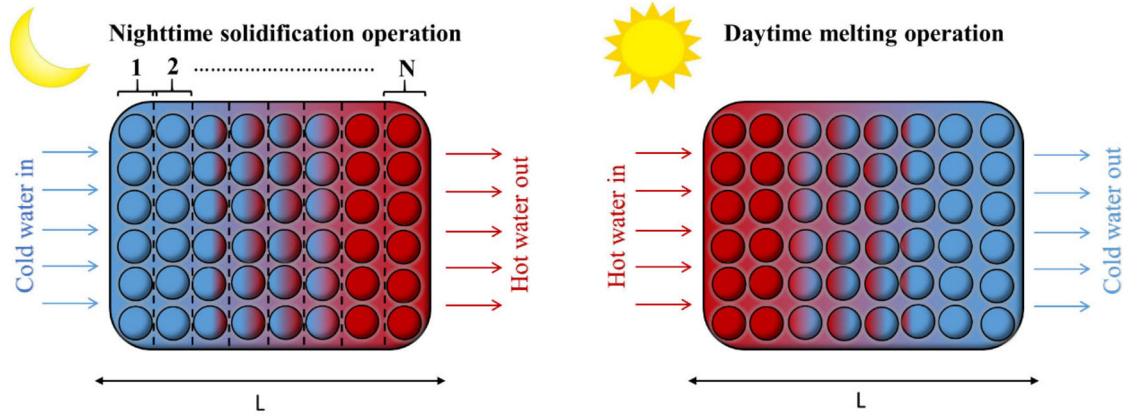


Fig. 4. Schematic of one PCM tank during solidification (nighttime) and melting (daytime).

radial direction is negligible; (5) the material constituting the PCM capsuled shell has a negligible thermal resistance.

Each tank is divided into N segments along its length. Each segment has the same height equal to the diameter of the capsules and contains one column having the same number of PCM as shown in Figure 4. Hence, the number of segments was fixed by dividing the length of the tank ($L = 1\text{ m}$) by the diameter of one spherical capsule which is equal to 5 cm. A simplified mathematical model is adopted to predict the temperature of the water and that of the PCM in each tank. The model is divided into two sub-models depending on the temperature of the PCM (T_{pcm}) (K).

1. Sub-model 1 is adopted when $T_{pcm} \neq T_{melting}$, and consists of solving the enthalpy change equation on each segment i of each storage tank. Based on assumption (5), the heat transfer between the water and the PCM capsules in each tank mainly happens through convection. The energy balance is shown in Equation (3) where the index j represents the tank about which the energy equation is applied $m_{pcm,j}$ (kg) and $N_{pcm,j}$ are respectively the mass of each PCM sphere and the number of PCM in each segment of tank j .

$$m_{pcm,j} N_{pcm,j} C_{p,pcm,j} \frac{dT_{pcm,j}(i)}{dt} = (T_{w,tank,j}(t,i) - T_{pcm,j}(t,i)) h_{pcm,j} A_{pcm,j} \quad (3)$$

The left side of Equation (3) represents the transient storage capacity of PCM in tank j which depends on the specific heat capacity of the PCM in tank j ($C_{p,pcm,j}$ (J/kg.K)). The right side represents the convective heat flow between the PCM in tank j and the water, this heat transfer method is highly affected by $h_{pcm,j}$ (W/m².K)– the heat transfer coefficient between the water and the PCM in tank j . $T_{w,tank,j}(t,i)$ (K) and $T_{pcm,j}(t,i)$ (K) are the temperatures of the water and the PCM in tank j at segment i and time t respectively, and $A_{pcm,j}$ (m²) is the total area of the PCM spheres in one segment of tank j .

2. Sub model 2 is adopted when $T_{pcm} = T_{melting}$. At this point, the PCM undergoes a phase change process modeled by Equation (4).

$$m_{pcm,j} L_{f,j} \frac{\partial f_{i,j}}{\partial t} = (T_{w,tank,j}(t,i) - T_{pcm,j}(t,i)) h_{pcm,j} A_{pcm,j} \quad (4)$$

where $f_{i,j}$ and $L_{f,j}$ (J/kg) are the melted fraction and the latent heat of fusion of PCM in the segment i of tank j , respectively.

As for the water flowing in the PCM tanks, the global conservation of energy in each segment of each tank is given by Equation (5). The left side of the equation designates the energy stored in the water. The first term of the right side represents the heat exchange between the water and the spherical capsules while the second term represents the net convective heat flow.

$$\begin{aligned} \rho_w V_{w,segment,j} C_{p,w} \frac{dT_{w,tank,j}}{dt} \\ = \dot{V}_{w,tank} \rho_w C_{p,w} (T_{w,tank,j}(t,i-1) - T_{w,tank,j}(t,i)) \\ - h_{pcm,j} A_{pcm,j} (T_{w,tank,j}(t,i) - T_{pcm,j}(t,i)) \end{aligned} \quad (5)$$

where $V_{w,segment,j}$ (m³) and $\dot{V}_{w,tank}$ (m³/s) are the volume of water in one segment of tank j and the volumetric flow rate of water flowing through the tanks, respectively.

3.3. The space model

The cooling load of the considered residence is calculated by developing a space model using the transient simulation software TRNSYS. (2019). Such software is known for its accurate estimation of building cooling load (Pagliarini, Corradi, and Rainieri 2012; Katramiz, Al-Jebaei, et al. 2020). The multi-zone building model type56 subroutine is employed to determine the cooling load in question. Furthermore, the energy rate mode is set with typical Kuwaiti indoor conditions: indoor air temperature of 23 °C and 50% relative humidity (Al-Rashidi, Loveday, and Al-Mutawa 2012). The model takes as input the physical and thermal properties of the building envelope, the internal gains as well as the weather data (Aviation Kuwait 2018). The architectural plan showing the dimensions of the rooms on the second floor of the considered building is shown in Figure 5.

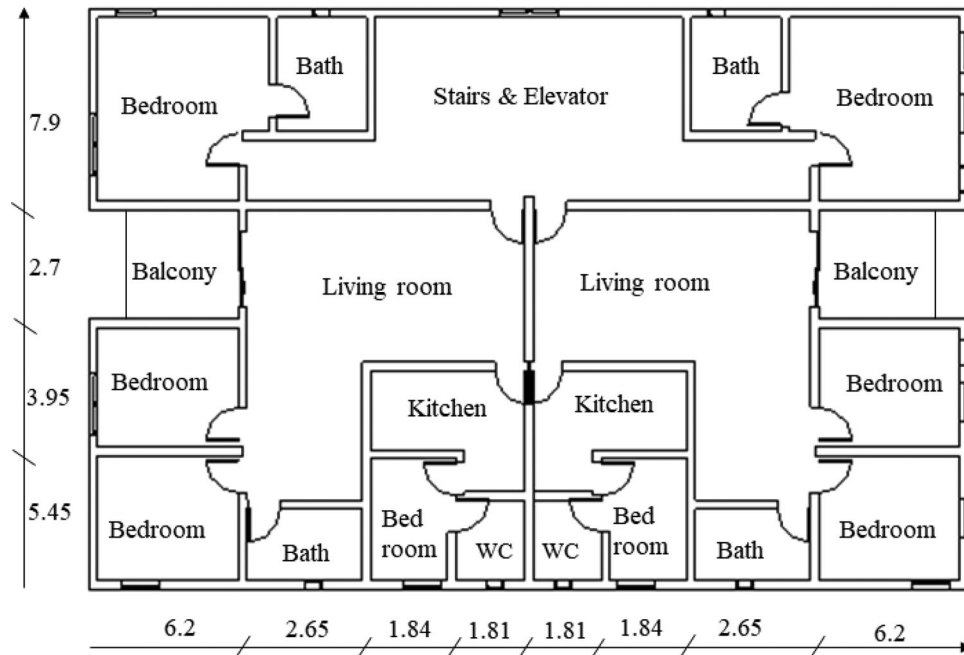


Fig. 5. Illustration of the architectural plan of the second floor of the studied residential house.

4. Numerical methodology

The operation of the integrated system is assessed by conducting numerical simulations following the chart presented in Figure 6. The space cooling load is first obtained for the entire Kuwaiti summer season using the simulation program TRNSYS. This software requires detailed information regarding the geometrical and thermal properties of the considered residential house, as well as the outdoor and indoor set conditions. The multi-zone building model type56 thus estimates the hourly cooling load of the residential house, which is set as input to the developed mathematical model in MATLAB. (2020) (Katramiz et al. 2021). The latter further requires additional input like the weather data, RC panel properties and PCM tanks properties. The simplified transient model consists of an implicit first-order time integration scheme, to solve the energy balance of the RC panel and PCM tank models. Note that a time step of 100s was adopted after conducting a time step independence test.

For each considered month, the initial fresh air flowrate ($\dot{m}_{fresh\ air}$) provided to the space is set to the minimum fresh air requirement recommended by ASHRAE (7.51/s/person) (ASHRAE. 2001). During each simulation, the following is conducted in the model: For nighttime operation, the fresh air is first cooled by heat recovery process in HE 1, and the resulting fresh air temperature $T_{f,a}$ is obtained. Then, the RC sub-model predicts the temperature of the water flowing through the panel ($T_{w,RC}$) by solving the corresponding differential equations iteratively. Based on $T_{w,RC}$, the solver checks whether the early or late night operation is needed to be simulated: if $T_{w,RC} > T_{m1}$, the early night operation is simulated as tank 2 is still charging while tank 1 is being used for air cooling; otherwise, tank 2 is completely solidified and tank 1 should start the charging process, and thus,

the late night operation starts. Accordingly, for each operation, the temperature of the water ($T_{w,tank}$) and PCM spheres (T_{pcm}) in tanks 1 and 2 are calculated via the PCM tank models, along with the temperature of the fresh air ($T_{f,a}$) leaving the water-air heat exchanger HE 2. Then, mixing between the fresh and return air is simulated to obtain the total supply air temperature $T_{a,AC}$ supplied to the AC unit for further cooling to meet the required nighttime cooling load of the space. For daytime operation, the RC sub-model is also used to determine the water temperature variation throughout the panel ($T_{w,RC}$), and the resulting fresh air temperature $T_{f,a}$ exiting HE 1 is obtained. Further air-cooling occurs in HE 2 due to the heat recovery process. Then, the water exiting PCM tank 1 is used to additionally cool the air in HE 3. Thus, using the PCM tank model, $T_{w,tank,1}$ and $T_{pcm,1}$ are predicted for tank 1, along with the resulting $T_{f,a}$ out of HE 3. Then mixing of the fresh air with the return air is simulated to get the total supply air temperature $T_{a,AC}$ supplied to the AC unit to reach eventually the required cooling load of the space. Note that during peak cooling hours of the day, the outdoor ambient air temperature (T_{amb}) is higher than the melting temperature of Tank 2 (T_{m2}), and the COP of the condenser is at its lowest, thus, PCM tank 2 is used to cool air entering the condenser ($T_{c,a}$). So $T_{w,tank,2}$ and $T_{pcm,2}$ are predicted via the PCM tank model, while $T_{c,a}$ resulting from the heat exchange with the water exiting tank 2 in HE 4 is obtained. Thus, the enhancement of the condenser COP is assessed for these specific peak hours.

To advance from one-time step to another in a simulation, a convergence criterion was set, where the difference between two consecutive iterations of any output parameter should be less than 10^{-5} . Note that simulations are repeated over a number of cycle days to reach a steady periodic

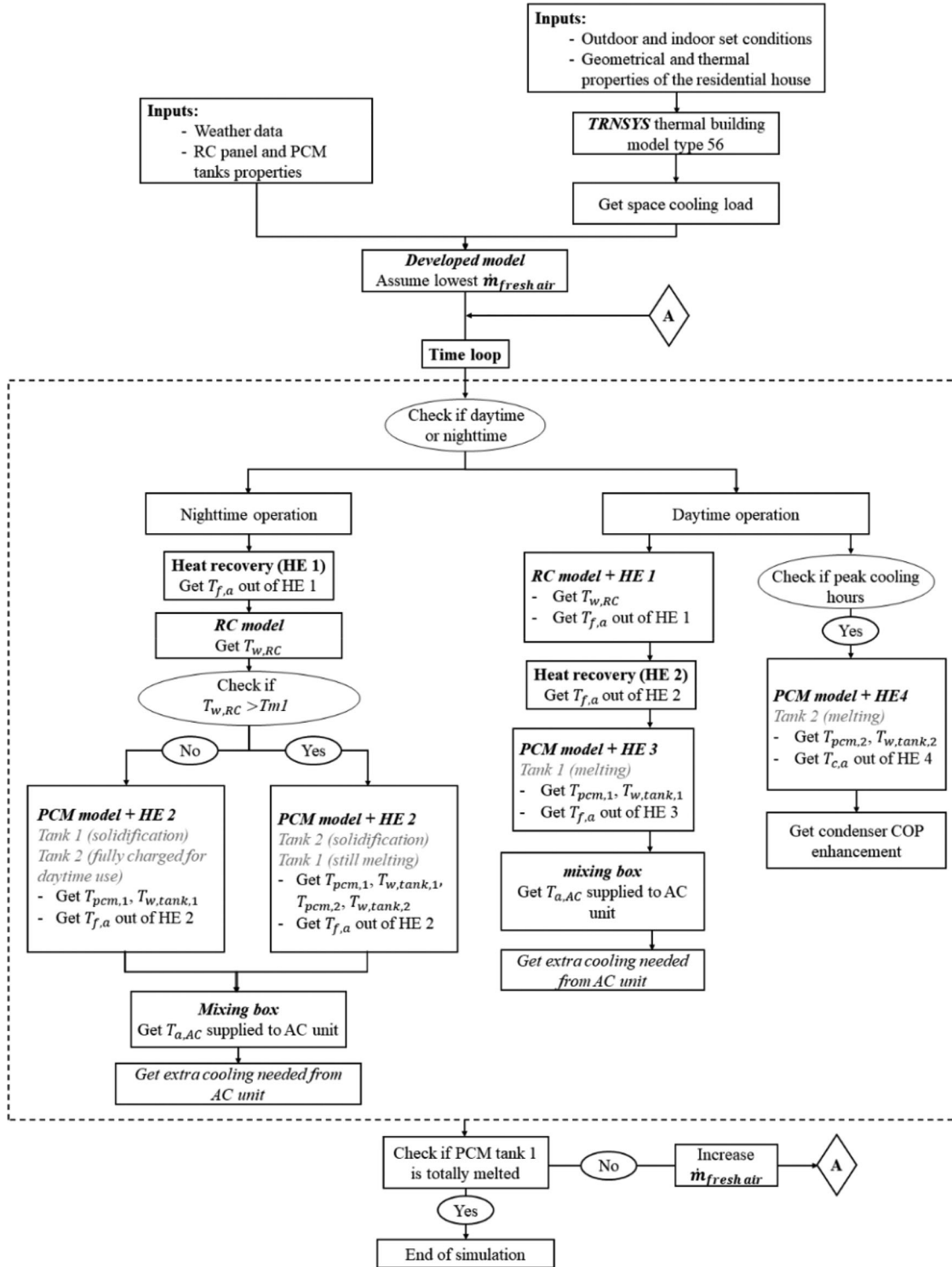


Fig. 6. Flow chart of the numerical modeling methodology.

solution. After reaching convergence, the solver checks the state of PCM tank 1: if this tank is totally melted at the end of the early night period, the simulation ends and the adopted $\dot{m}_{fresh\ air}$ is adequate; otherwise, $\dot{m}_{fresh\ air}$ is increased, and the simulation is repeated. Thus, the amount of fresh air increase provided by the proposed system operation is assessed.

5. Description of the case study

In order to assess the performance of the proposed system, a typical Kuwait building is investigated for the entire cooling season: April through October. ASHRAE standard 169-2013 (2013) categorized the countries based on their climate specifications. Based on this standard, Kuwait is considered a

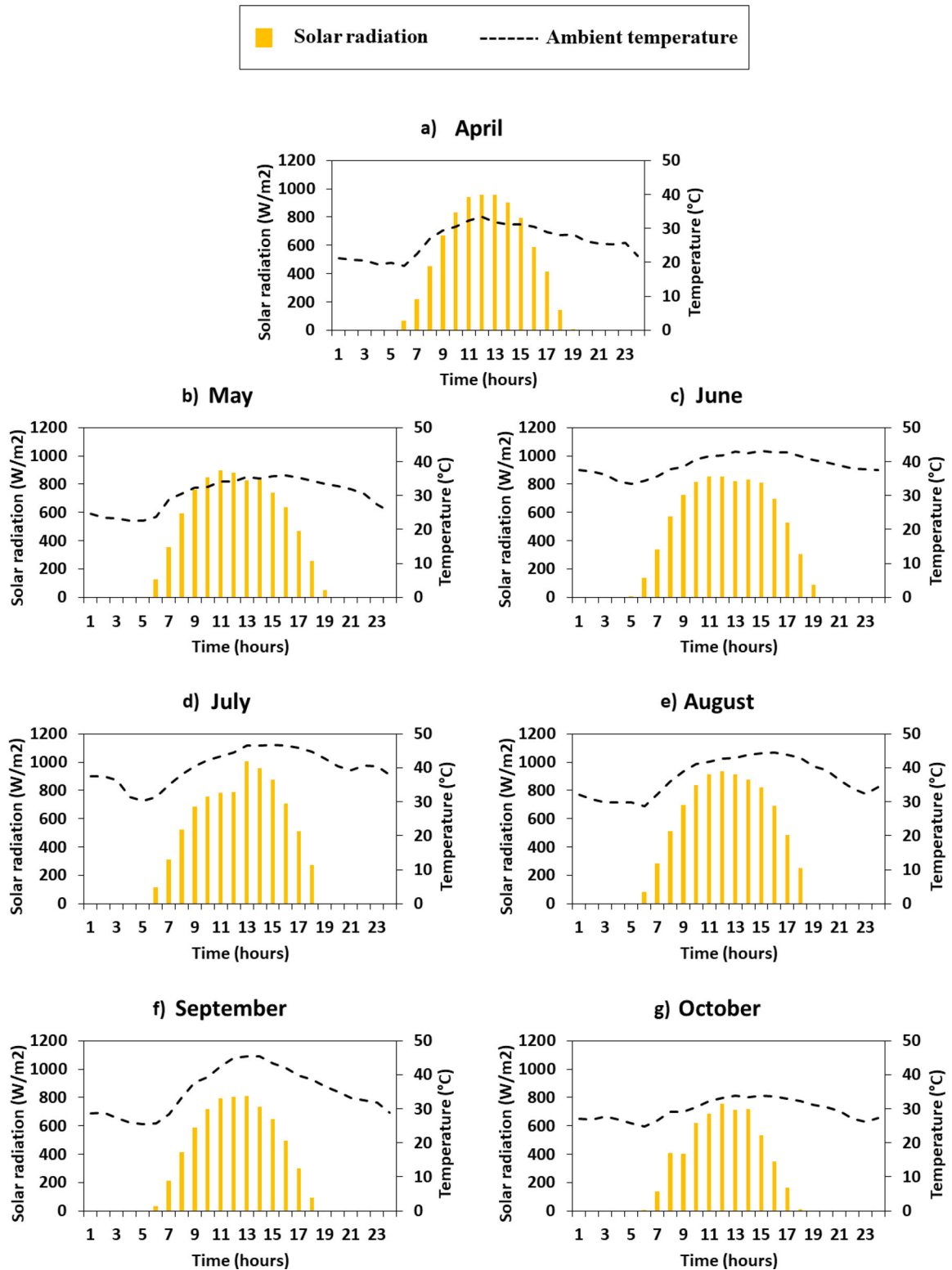


Fig. 7. Hourly variation of temperature and solar radiation for a representative day of each cooling month.

hot and dry country that belongs to category 0B, where 0 means extremely high temperature area and B means dry area. The proposed system can be applied to other countries belonging to categories considering dry climates (1B - very hot and dry, 2B - hot and dry, and 3B - warm and dry). In

fact, dry conditions are necessary for the efficient performance of the RC panel. The weather data for each considered month is obtained from the Kuwait Meteorological Center (2020). Figure 7 shows the ambient temperature and solar radiation for the representative day of each summer month.

Table 1. Thermal details of the envelope layers (inside to outside).

Layer	Thickness (mm)	Density (kg/m ³)	C _p (kJ/kg·K)	RSI-Value (m ² ·K/W)
Inside surface resistance	–	–	–	0.1206
102mm LW concrete block	102	608.7	0.837	0.2668
RSI-1.2 board insulation	25.4	32.04	0.921	1.2229
203mm common brick	203	1922.22	0.837	0.2795
203mm HW concrete	203	2242.58	0.837	0.1174
Outside surface resistance	–	–	–	0.0586

Furthermore, the relative humidity ranged between 10% and 60% throughout the cooling season.

The considered building is a two-story residential house of height 13.65 m, each floor having a surface area of (25 m × 20 m). The considered residential villa is divided into four zones: the living room, the bedroom, the kitchen and the bathrooms. The physical composition of the space envelope is presented in Table 1. As for the windows, the glazing U-value is set to 3.33 w/m²·K and SHGC is 0.36 (Ministry of Electricity and Water MEW/R-6 2016). The residential house is considered occupied by six people, each having a sensible load of 75 W and a latent load of 55 W. Internal heat gains account for occupants, electrical equipment and lights in the residence. Appliances and electrical equipment that were considered in the house under study are: Refrigerator (800 W), water cooler (150 W), microwave oven (1000 W), two laptops (50 W each) and three televisions (130 W each) (Ameer and Krarti 2016). The infiltration rate was taken to be 0.2 ACH adopted from a study by Bouhamra, Elkilani, and Abdul-Raheem (1998) who assessed air exchanges rates in Kuwaiti residences. As for the PCM storage tanks, they are fully insulated water/PCM tanks. The PCM is placed inside highly conductive spherical capsules. When the temperature of the water surrounding the PCM spheres is low, they solidify while releasing their energy to the water. Otherwise, the PCM spheres melt as they absorb heat from the surrounding water. The PCM melting temperature used in each tank should be set based on the available cooling power produced by the RC panel during the nighttime period. Thus, this is chosen after conducting simulations and is presented in the system sizing section. Furthermore, the material of the RC panel reported in the study of Bao et al. (2017) is adopted in this work, due to its meaningful daytime radiative cooling, its scalable coating that has significant potential in large scale applications at a relatively low cost. It consisted of a double-layer nanoparticle-based coating structure. The double layer-coatings are on top of an aluminum substrate and are composed of a reflective layer on top of an emissive layer. The reflective material is chosen to be a common material with stable chemical properties and high refractive index: titanium dioxide (TiO₂), with a thickness of 25 μm. The latter is highly reflective in the solar spectrum and transparent in the mid infrared spectrum. Silicon dioxide (SiO₂) is chosen to

achieve selective emission in the “transparency window” with a thickness of 20 μm.

6. Results and discussion

In this section, the integrated model validation of the hybrid RC-PCM and AC system is presented followed by the results of the system sizing for the case study of the typical Kuwaiti residence. The system operation is analyzed over the entire cooling months to present the increase in fresh air supply over the conventional system as well as the energy savings associated with the system implementation.

6.1. Model validation

The developed model in this work is an integration of previously validated and well-documented models in literature (Bao et al. 2017; Ismail and Henriques 2002). The temperature decrease below ambient achieved by the RC panel model was compared to the experimentally validated model of Bao et al. (2017). For validation purposes, the developed RC model of this work was used in combination with the assumptions and boundary conditions (climatic conditions, geometry of the panels) considered by Bao et al. (2017): a solar radiation of 860 W/m², an average air temperature of 20 °C and a convective coefficient between the surface of the panel and the ambient air of 6.9 W/m²·K. While comparing the results obtained for the temperature decrease from the developed RC model with the results reported by Bao et al. (2017), a maximum error of 5.8% was observed. As for the water/PCM tank model, it was validated with the model of Ismail and Henriques (2002). The same assumptions and boundary conditions considered by Ismail and Henriques (2002) were used as inputs to the developed PCM tank model: a spherical capsule diameter of 77 mm, a melting temperature of 20 °C, a working fluid temperature of –3 °C and a flow rate of 0.5 m³/h. While comparing the numerical findings with the experimental of Ismail and Henriques (2002), a maximum error of 7.2% was reported.

6.2. System sizing

To ensure the successful operation of the proposed system, it is crucial to properly size its different components. For the RC panel sizing, it is well established that the increase in

Table 2. Characteristics of the PCM storage tanks.

	Tank 1	Tank 2
Name of material	RT22HC Paraffin	RT28HC paraffin
PCM melting temperature [$^{\circ}\text{C}$]	22	28
Latent heat of fusion L_f [kJ/kg]	250	190
Specific heat capacity C_{pcm} [kJ/kg·K]	2	2
Density [kg/m^3]	800	750
Total mass [kg]	160	200
Width [m]	0.45	0.50
Length [m]	2	2
High [m]	0.45	0.5

the area of the panel increases its cooling capacity. Thus, in this work, a maximum RC panel area was set to cover 70% of the roof. Note that the remaining area is dedicated for other system components as storage tanks. The resulting water temperature leaving the RC panel $T_{w,RC}$ during nighttime period varied between 28°C during early night hours and around 16°C at the end of the night period. Subsequently, the melting temperatures of the PCM tanks were fixed according to $T_{w,RC}$:

- Since PCM tank 1 is used to further cool the fresh air that has already harvested the cooling power of the exhaust air by heat recovery, the melting temperature of the PCM in tank 1 must be lower than that of the exhaust air (i.e. lower than around 24°C). Thus, T_{m1} must be between 24°C and 16°C (lowest $T_{w,RC}$). RT22HC paraffin was therefore chosen for tank 1 as the low melting temperature PCM, with T_{m1} of 22°C .
- On the other hand, the melting temperature of PCM tank 2 should be selected based on $T_{w,RC}$ during the early night hours. As a result, RT28HC paraffin was used in storage tank 2, with a high melting temperature T_{m2} of 28°C .

These PCMs are commercially available by Rubitherm. As for the PCM storage tanks, they were sized to be able to harvest all the cooling power produced by the RC panel during nighttime. Since the performance of the RC panel is highly affected by the outdoor conditions (ambient temperature, relative humidity, solar radiation etc.), the sizing of the system should be designed according to the peak summer month. Thus, the cooling loads for each month were obtained using TRNSYS, and benchmarked with reported cooling load data in literature for Kuwaiti residences (Al-Ajmi and Hanby 2008). As a result, July was found to be the month with the peak cooling loads, ranging between a minimum of $17\text{W}/\text{m}^2$ during nighttime and a maximum of $38\text{W}/\text{m}^2$ during daytime. Accordingly, the sizing of each PCM storage tank was based on the weather data of July. The flow rate of the air supplied to the space was fixed to $4\text{m}^3/\text{s}$ (Katramiz, Al-Jebaei, et al. 2020). After running many simulations to obtain the lowest water temperature at the exit of the RC panel during the month of July, the flow rate of water flowing in the RC loop was set to $0.181/\text{s}$. During July, the PCM spheres in tank 1 started solidifying at late hours of the night (around 1:00 A.M) when the

temperature of the water out of the panels was lower than T_{m1} (22°C). Thus, the needed PCM mass in tank 1 was fixed based on the cooling power of the RC panel from 1:00 A.M until the end of the nighttime period (around 6:00 A.M). As for the PCM spheres in tank 2, they should undergo solidification during early nighttime hours (around 7:00 P.M) when the temperature of the water exiting the RC panel is lower than T_{m2} (28°C). Note that the size of tank 2 was fixed based on the cooling load provided by the RC panel during early nighttime period, i.e., before the temperature of the water exiting the RC panel was lower than T_{m1} . Accordingly, the PCM storage tanks were adequately sized: each tank is totally melted at the end of its corresponding operation schedule, with the PCM spheres reaching their melting temperature (T_{m1} and T_{m2} respectively). This sizing strategy ensures that the RC power is only used to solidify the PCM storage tanks. The operational parameters as well as the thermos-physical properties of each PCM are presented in Table 2.

6.3. System operation

After sizing the system, its operation was assessed for the entire cooling season by conducting simulations using the developed model. The nocturnal cooling power of the RC panel was harvested in two PCM storage tanks: tank1 having the lowest melting temperature ($T_{m1} = 22^{\circ}\text{C}$) and tank 2 having the highest melting temperature ($T_{m2} = 28^{\circ}\text{C}$). The cooling power stored in both tanks is used for two different operations during daytime both aiming at reducing the energy consumption of the AC system and maintaining an acceptable indoor air temperature of 23°C . These operation modes mainly rely on the outdoor conditions which define the water temperature out of the RC panels. In fact, during the peak month of July, the temperature of the water out of the RC panel at the beginning of the night (at 7:00 P.M) reaches values as high as 28°C . This water will enter tank 2 and cold energy will be stored while solidifying the PCM spheres. Throughout the night, the water out of the RC panel will keep charging tank 2 until the water temperature exiting the RC panels reaches values lower than T_{m1} at 12:00 midnight approximately. At that moment, the water will enter tank1 and the cooling power will be stored at low temperature by solidifying the PCM. During daytime (from 6:00 A.M till 7:00 P.M), the temperature of the water leaving

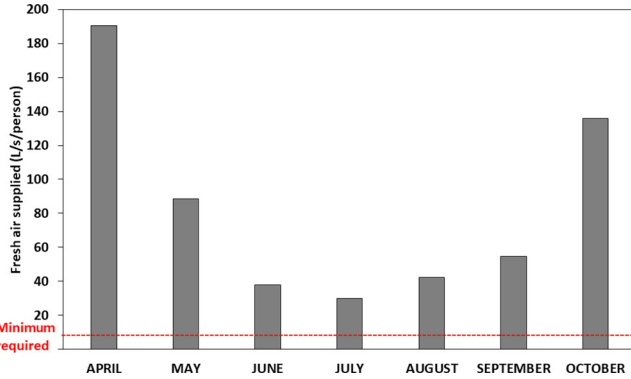


Fig. 8. Flow rate of fresh air supplied to the space for the entire cooling season.

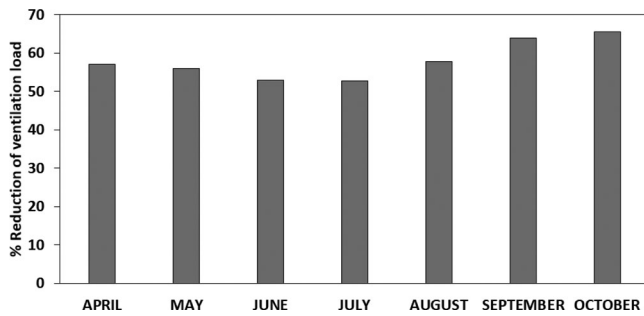


Fig. 9. Percentage (%) of the monthly ventilation load reduction for the entire cooling season.

the RC panel increases from 16°C at the beginning of the day until reaching values as high as 30°C at around 2:00 P.M. This water will be used as a first-stage precooling of the fresh air during daytime: the fresh air at high temperatures (between 31°C and 44°C) will exchange heat with the water out of the RC panel. At the second stage, the fresh air undergoes further cooling by exchanging heat with the air exhausted from the villa at around 24°C. The last stage consists of heat exchange between the air (ideally at 24°C) and the water exiting PCM tank 1 at temperature around T_{m1} . The pre-cooled air then enters the AC unit if further cooling is needed.

As previously mentioned, PCM tank 1 was integrated with the RC panel to pre-cool the fresh air. This provided the opportunity to increase the amount of fresh air supplied to the space, with zero energy consumption compared to the conventional AC system. Figure 8 presents the fresh air flowrate per person ($\dot{m}_{fresh\ air}$) supplied to the space, which exceeded the minimum requirements of 7.5 l/s/person (ASHRAE, 2001) for all the summer months. Note that for each considered summer month, $\dot{m}_{fresh\ air}$ was maintained constant throughout the day, and that the entire ventilation load was met by the proposed passive system. The smallest amount of fresh air supplied to the space (30 l/s/person) was observed for the peak month of the cooling season (i.e. July): four times higher than the minimum required amount. This portion of fresh air increased for the moderate months until reaching 190 l/s/person, exceeding the minimum required amount by twenty-five times for the month of

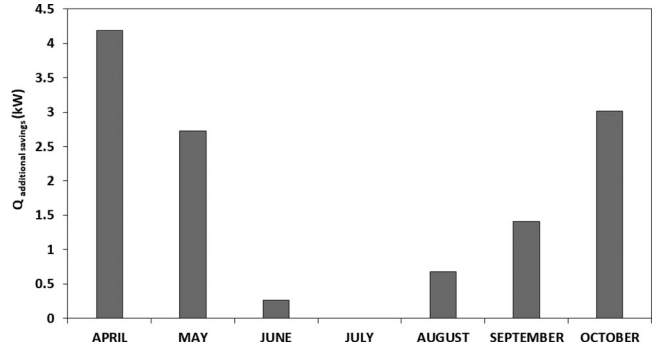


Fig. 10. Average additional savings in the electric loads due to cooling for a representative day of the cooling season.

April. This was predictable due to the relatively low outdoor conditions during this month (Figure 7a).

The proposed system was able to meet the entire ventilation load for all the considered months based on the corresponding $\dot{m}_{fresh\ air}$ (Figure 8). The percentage ventilation savings of the proposed system with respect to the conventional AC system with heat recovery, for the same fresh air intake is presented in Figure 9. In order to get the same IAQ relying only on the conventional AC system, an average ventilation load of 0.95 kW will be required per day for the entire cooling season. This required load was completely met by the proposed system. An average of 58% of total ventilation load reduction was achieved during the entire Kuwaiti summer season, with a maximum of 65.5% for the month of October followed by 63.8% for September, 57.8% for August, 57.1% for April, 56% for May, 53% for June and a minimum of 52.7% for the peak month of July.

Furthermore, for the off-peak months, the system was capable of reducing the fresh air temperature to the AC below that of the return air (T_{return}). This reduction was mostly observed when the RC cooling power was high enough, especially in moderate climate conditions. The resultant mixture of return and fresh air (\dot{m}_{supply}) was thus at a temperature $T_{a,AC}$ less than T_{return} . Additional savings in the AC system electric loads for cooling were consequently achieved. These savings were calculated using equation (6):

$$Q_{additional\ saving} = \dot{m}_{supply} C_{p,a} (T_{return} - T_{a,AC}) \quad (6)$$

Figure 10 shows the average additional savings in the electric loads for a representative day of each considered summer month. As predicted, for the peak month of July, the system was only capable of meeting the ventilation load, and no additional savings were reported. Whereas, for the remaining months, the system was able to provide considerable additional savings, with a maximum of 4.1 kW for the month of April. Note that the trend of variation of $Q_{ventilation\ savings}$ and $Q_{additional\ savings}$ between the summer months followed that of fresh air intake (Figure 8). An average of 2 kW additional electrical load savings was therefore achieved daily during the entire Kuwaiti summer season.

The use of tank 1 was able to enhance the performance of the AC system by meeting the ventilation load and procuring additional savings in the electrical cooling loads.

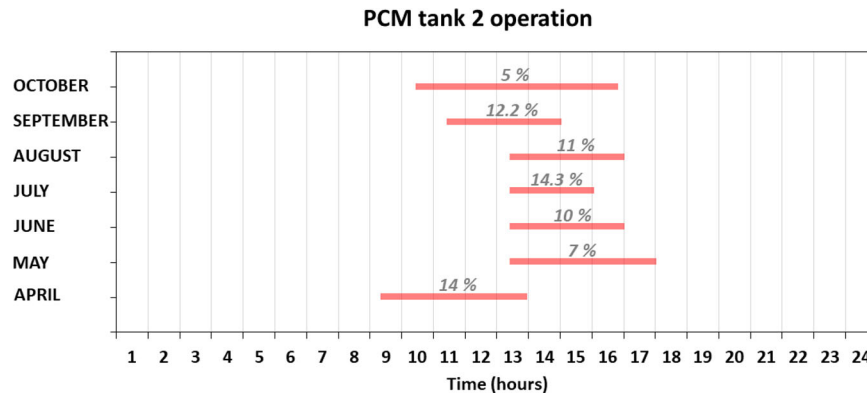


Fig. 11. Hourly schedule of the PCM tank 2 operation and corresponding percentage of COP enhancement for each considered summer month.

Further enhancement can be achieved by using the cold power stored in PCM tank 2 to cool the ambient air entering the condenser of the AC unit during the peak daytime hours. In fact, the ambient air temperature highly affects the COP of an air-cooled condenser (Hajidavalloo and Eghtedari 2010). Motta and Domanski (2000) investigated the effect of pre-cooling the air entering the condenser on the COP of an AC system having similar specifications and cooling loads as the one adopted in this work. They reported a correlation between the COP and ambient temperature for a range of [25 °C–50 °C]. Note that the air temperature of the considered Kuwaiti summer months falls within that range. Thus, this correlation was adopted in this work to assess the effect of air cooling on the COP of the system and resulting energy savings. Figure 11 shows the hourly schedule of the PCM tank 2 operation and corresponding COP enhancement percentage for each considered summer month. The operation schedule of tank 2 varied from month to another, as it depends on two parameters: the peak hours period during which the COP was at its lowest, as well as the difference between the ambient temperature (T_{amb}) and the melting temperature of tank 2 (T_{m2}). As expected, the maximum COP enhancement was achieved during the peak month of July: T_{amb} was largely exceeding T_{m2} (28 °C), which induced a 14.3% COP enhancement for a period of around 3 hours (between 13:00 P.M and 16:00 P.M), until the total melting of tank 2. This percentage decreased for the moderate months, where T_{amb} was closer to T_{m2} . Thus, the lowest COP enhancement was obtained for the month of October (5%), however with a long operation period of around 6 hours until the depletion of the cooling power of PCM tank 2 (i.e. total melting of the PCM).

6.4. Energy saving analysis

In this study, the performance of the AC system was enhanced due to the implementation of the proposed system. The usage of tank 1 helped in reducing the electrical cooling load required from the mechanical cooling system q_L : the entire ventilation load was met compared to the conventional AC system and additional savings were achieved during off-peak months (Figure 10). On the other hand, tank 2 was able to enhance the COP by cooling the ambient air entering

the condenser. The combination of those two operations resulted in a remarkable decrease in the total energy consumption of the AC system which was assessed by the following equation:

$$E = \frac{q_L}{COP} \quad (6)$$

where E and q_L are the total energy consumption of the AC system and the electrical cooling load required from the mechanical cooling system, respectively. Figure 12 shows the percentage of the total energy consumption reduction for the Kuwaiti entire cooling season in comparison to the case when the same $\dot{m}_{fresh\ air}$ was treated by the conventional AC system. An average of 22.2% reduction in energy consumption was found for the entire considered cooling season, with a maximum of 39% in April due to its moderate weather conditions that improved the performance of the RC panel and led to an enhancement in the overall system effectiveness. However, a minimum of 6.7% was observed for the peak summer month of July where the outdoor conditions were extremely high.

7. Limitations and applicability

The proposed assistive passive cooling system was implemented in the hot and dry climate of Kuwait, yielding high performance levels of the RC panels and meeting the ventilation load of the residential building. However, such advantageous operation cannot be reached under other climate conditions. In fact, the proposed system shows to be less effective when implemented in humid climates as this will decline the performance of the RC panels (Zhao, Aili, et al. 2019). This is because the spectral transmittance of the atmosphere is largely affected by the humidity of the air: a high relative humidity (RH) will cause lower transmittance to the outer space and decrease the RC panels cooling potential (Parker 2005). Consequently, extensive studies must be executed to know whether this reduction in ambient temperature can compensate the increase in RH.

On the other hands, other aspects of weather conditions should be considered when implementing this system.

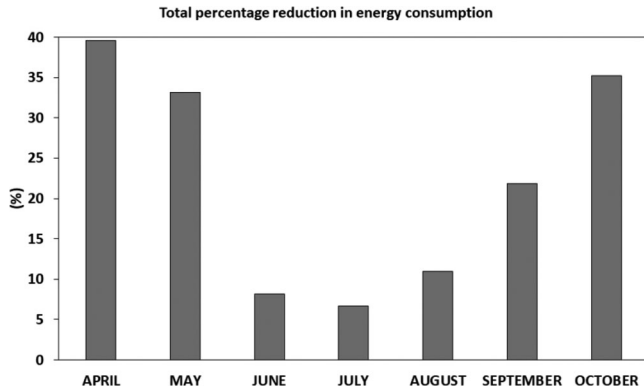


Fig. 12. Average percentage reduction of the energy consumption using the proposed system with respect to the conventional mechanical cooling system for the entire summer season.

Kuwait is known for its hazardous weather conditions characterized by a high occurrence of sand and dust storm (AlKheder and AlKandari 2020; Furman 2003), especially during the summer seasons (Sabbah et al. 2018). During dusty days, the wind speed showed a considerable increase, which jeopardize the performance of the RC panels (Zhao, Aili, et al. 2019). In addition, the dust particles can scatter the sun rays back to the outer space decreasing by that the ambient air temperature during dusty days (Sabbah et al. 2018). Moreover, RC panels require a recurrent cleaning method to ensure their maximum performance by ensuring the intactness of the panel's nanomaterials.

Finally, in this study, the system was implemented for a residential building application, where there is need for cooling during both night and day period due to the presence of occupants. However, it is of great importance to extend the application of such system for other building types (like classrooms, office spaces, restaurants, etc.) that have different occupancy schedules than residential buildings. This will result in a different system operation strategy as there will be no cooling load that needs to be offset during nighttime (non-occupied period). Consequently, the proposed system will be more effective since the entire nocturnal cooling power of the RC panels that is harvested by the PCM tanks will be used during daytime period for enhancing the performance of the mechanical cooling system.

8. Conclusion

This paper evaluated the integration of a passive cooling system composed of a RC panel combined with two PCM storage tanks to assist the mechanical AC system in meeting the cooling load of a typical Kuwaiti residential building. The nocturnal cooling power of the RC panel was stored in two PCM storage tanks, having low and high melting temperature respectively. The low temperature PCM tank (tank 1) was used to cool the fresh air supplied to the space, and the high temperature PCM tank (tank 2) was implemented to enhance the COP of the AC system by cooling the air entering its condenser. A mathematical model was thus developed

to assess the system performance for the entire Kuwaiti cooling period extending from April to October. It was found that the use of tank 1 helped in increasing the fresh air ventilation rate at zero energy cost, while minimizing the intervention of the mechanical AC system. Furthermore, the implementation of tank 2 led to an increase of the COP by an average of 10.5%. The proposed system was hence able to decrease the overall energy consumption by 22.2% with respect to the conventional AC system providing the same IAQ. This highlights the beneficial role of integrating the proposed passive system to assist the AC system in offsetting the increase in energy consumption related to the conditioning of the high temperature fresh air intake and providing high IAQ levels in the hot climate of Kuwait.

Disclosure Statement

No potential conflict of interest was reported by the author(s).

Funding

The authors would like to acknowledge the Kuwait Foundation for the Advancement of Sciences (KFAS) for supporting this research grant number: AP1835EM01.

References

- Ahmad, M. I., H. Jarimi, and S. Riffat. 2019. *Nocturnal cooling technology for building applications*. Singapore: Springer.
- Al Touma, A., K. Ghali, N. Ghaddar, and N. Ismail. 2016. Solar chimney integrated with passive evaporative cooler applied on glazing surfaces. *Energy* 115:169–79. doi:10.1016/j.energy.2016.09.020
- Al-Ajmi, F. F., and V. Hanby. 2008. Simulation of energy consumption for Kuwaiti domestic buildings. *Energy and Buildings* 40 (6): 1101–9. doi:10.1016/j.enbuild.2007.10.010
- AlKheder, S., and A. AlKandari. 2020. The impact of dust on Kuwait International Airport operations: A case study. *International Journal of Environmental Science & Technology (IJEST)* 17 (7): 3467–3474.
- Alotaibi, S. 2011. Energy consumption in Kuwait: Prospects and future approaches. *Energy Policy* 39 (2):637–43. doi:10.1016/j.enpol.2010.10.036
- Al-Rashidi, K., D. Loveday, and N. Al-Mutawa. 2012. Impact of ventilation modes on carbon dioxide concentration levels in Kuwait classrooms. *Energy and Buildings* 47:540–9. doi:10.1016/j.enbuild.2011.12.030
- Ameer, B., and M. Krarti. 2016. Impact of subsidization on high energy performance designs for Kuwaiti residential buildings. *Energy and Buildings* 116:249–62. doi:10.1016/j.enbuild.2016.01.018
- ASHRAE. 2001. *ANSI/ASHRAE Standard 62-2001 Ventilation for acceptable indoor air quality*. Atlanta: ASHRAE.
- Aviation-Kuwait. 2018. D.G.o.C. Meteorological Department. Available from: <https://www.met.gov.kw/>.
- Baakeem, S. S., J. Orfi, A. Mohamad, and S. Bawazeer. 2019. The possibility of using a novel dew point air cooling system (M-Cycle) for A/C application in Arab Gulf Countries. *Building and Environment* 148:185–97. doi:10.1016/j.buildenv.2018.11.002

- Bao, H., C. Yan, B. Wang, B. Fang, C. Y. Zhao, and X. Ruan. 2017. Double-layer nanoparticle-based coatings for efficient terrestrial radiative cooling. *Solar Energy Materials and Solar Cells* 168: 78–84. doi:10.1016/j.solmat.2017.04.020
- Bouhamra, W. S., A. S. Elkilani, and M. Y. Abdul-Raheem. 1998. Predicted and measured air exchange rates. *ASHRAE Journal-American Society of Heating Refrigerating and Airconditioning Engineers* 40 (8):42–5.
- Dai, H., and B. Zhao. 2020. Association of the infection probability of COVID-19 with ventilation rates in confined spaces. *Building Simulation* 13 (6):1321–7.
- Dutil, Y., D. Rousse, N. B. Salah, S. Lassue, and L. Zalewski. 2011. A review on phase-change materials: Mathematical modeling and simulations. *Renewable and Sustainable Energy Reviews* 15 (1): 112–30. doi:10.1016/j.rser.2010.06.011
- Furman, H. K. H. 2003. Dust storms in the Middle East: Sources of origin and their temporal characteristics. *Indoor and Built Environment* 2003. 12 (6):419–26. doi:10.1177/1420326X03037110
- Gentle, A. R., and G. B. Smith. 2010. Radiative heat pumping from the earth using surface phonon resonant nanoparticles. *Nano Letters* 10 (2):373–9. doi:10.1021/nl903271d
- Hajidavalloo, E., and H. Eghtedari. 2010. Performance improvement of air-cooled refrigeration system by using evaporatively cooled air condenser. *International Journal of Refrigeration* 33 (5):982–8. doi:10.1016/j.ijrefrig.2010.02.001
- Harrouz, J. P., K. Ghali, and N. Ghaddar. 2021. Integrated solar-Windcatcher with dew-point indirect evaporative cooler for classrooms. *Applied Thermal Engineering* 188:116654. doi:10.1016/j.applthermaleng.2021.116654
- Head, A. K. 1962. Method and means for producing refrigeration by selective radiation, US3043112A, submitted February 9, 1959.
- Hu, M., Y. Su, J. Darkwa, and S. Riffat. 2020. Implementation of passive radiative cooling technology in buildings: A review. *Buildings* 10 (12):215. doi:10.3390/buildings10120215
- Ismail, K. A. R., and J. R. Henri 'quez. 2002. Numerical and experimental study of spherical capsules packed bed latent heat storage system. *Applied Thermal Engineering* 22 (15):1705–16. doi:10.1016/S1359-4311(02)00080-7
- Jeong, S. Y., C. Y. Tso, M. Zouagui, Y. M. Wong, and C. Y. H. Chao. 2018. A numerical study of daytime passive radiative coolers for space cooling in buildings. in. *Building Simulation* 11 (5): 1011–28. doi:10.1007/s12273-018-0474-4
- Jeong, S. Y., T. C. Wong, Y. M. Chao, and C. Y. 2018. Passive radiative cooler based on biomimetic metasurface from Saharan silver ants. Proceedings of the 4th International Conference on Building Energy and Environment. Melbourne, Australia
- Katramiz, E., H. Al-Jebaei, S. Alotaibi, W. Chakroun, N. Ghaddar, and K. Ghali. 2020. Sustainable cooling system for Kuwait hot climate combining diurnal radiative cooling and indirect evaporative cooling system. *Energy* 213:119045. doi:10.1016/j.energy.2020.119045
- Katramiz, E., N. Ghaddar, and K. Ghali. 2020. Daytime radiative cooling: To what extent it enhances office cooling system performance in comparison to night cooling in semi-arid climate? *Journal of Building Engineering* 28:101020. doi:10.1016/j.job.2019.101020
- Katramiz, E., N. Ghaddar, K. Ghali, D. Al-Assaad, and S. Ghani. 2021. Effect of individually controlled personalized ventilation on cross-contamination due to respiratory activities. *Building and Environment* 194:107719. doi:10.1016/j.buildenv.2021.107719
- Kauranen, P., K. Peippo, and P. Lund. 1991. An organic PCM storage system with adjustable melting temperature. *Solar Energy* 46 (5): 275–8. doi:10.1016/0038-092X(91)90094-D
- Kellow, M. 1989. Kuwait's approach to mandatory energy-conservation standards for buildings. *Energy* 14 (8):491–502. doi:10.1016/0360-5442(89)90115-1
- Kuwait Meteorological Center. 2020. From <https://www.met.gov.kw/>.
- Li, Y., G. M. Leung, J. W. Tang, X. Yang, C. Y. Chao, J. Z. Lin, J. W. Lu, P. V. Nielsen, J. Niu, H. Qian, et al. 2007. Role of ventilation in airborne transmission of infectious agents in the built environment – a multidisciplinary systematic review. *Indoor Air* 17 (1):2–18. doi:10.1111/j.1600-0668.2006.00445.x
- MATLAB. 2020. Mathworks Version: R2020b. Available from: <https://www.mathworks.com/products/matlab.html>
- Meir, M., J. B. Rekestad, and O.M. Løvrvik. 2002. A study of a polymer-based radiative cooling system. *Solar Energy* 73 (6): 403–417. doi: 10.1016/S0038-092X(03)00019-7
- Mihalakakou, G., A. Ferrante, and J. Lewis. 1998. The cooling potential of a metallic nocturnal radiator. *Energy and Buildings* 28 (3):251–6. doi:10.1016/S0378-7788(98)00006-1
- Ministry of Electricity and Water MEW/R-6. 2016. Code of practice. Available from: https://kupdf.net/download/mew-r6-2016_59d22da308bbc57429686f94_pdf.
- Motta, S. Y., and P. A. Domanski. 2000. Performance of R-22 and its alternatives working at high outdoor temperatures. Proceedings of International Refrigeration and Air Conditioning Conference, Paper 464. Purdue University, USA. <http://docs.lib.purdue.edu/iracc/464>.
- Oguntala, G., G. Sobamowo, and R. Abd-Alhameed. 2019. Numerical analysis of transient response of convective-radiative cooling fin with convective tip under magnetic field for reliable thermal management of electronic systems. *Thermal Science and Engineering Progress* 9:289–98. doi:10.1016/j.tsep.2018.12.005
- Orel, B., M. K. Gunde, and A. Krainer. 1993. Radiative cooling efficiency of white pigmented paints. *Solar Energy* 50 (6) :477–82. doi:10.1016/0038-092X(93)90108-Z
- Pagliarini, G., C. Corradi, and S. Rainieri. 2012. Hospital CHCP system optimization assisted by TRNSYS building energy simulation tool. *Applied Thermal Engineering* 44:150–8. doi:10.1016/j.applthermaleng.2012.04.001
- Park, J., T. Kim, and C-s Lee. 2019. Development of thermal comfort-based controller and potential reduction of the cooling energy consumption of a residential building in Kuwait. *Energies* 12 (17): 3348. doi:10.3390/en12173348
- Parker, D. S. 2005. *Theoretical evaluation of the night cool nocturnal radiation cooling concept*. Submitted to: US Department of Energy. FSEC-CR-1502-05.
- Rubitherm. 2021. Rubitherm Inc., Phase Change Material. Available from: <https://www.rubitherm.eu/en/index.php/productcategory/organische-pcm-rt>.
- Sabbah, I., J.-F. Léon, M. Sorribas, B. Guinot, C. Córdoba-Jabonero, A. de Souza, and F. Al Sharifi. 2018. *Dust and dust storms over Kuwait: Ground-based and satellite observations*. *Journal of Atmospheric and Solar-Terrestrial Physics* 179:105–13. doi:10.1016/j.jastp.2018.06.006
- Safaei, M. R., H. R. Goshayeshi, and I. Chaer. 2019. Solar still efficiency enhancement by using graphene oxide/paraffin nano-PCM. *Energies* 12 (10):2002. doi:10.3390/en12102002
- Sarafraz, M., M. R. Safaei, A. S. Leon, I. Tlili, T. A. Alkanhal, Z. Tian, M. Goodarzi, and M. Arjomandi. 2019. Experimental investigation on thermal performance of a PV/T-PCM (photovoltaic/thermal) system cooling with a PCM and nanofluid. *Energies* 12 (13):2572. doi:10.3390/en12132572
- Shahsavari, A., S. Khanmohammadi, A. Karimipour, and M. Goodarzi. 2019. A novel comprehensive experimental study concerned synthesizes and prepare liquid paraffin-Fe3O4 mixture to develop models for both thermal conductivity & viscosity: A new approach of GMDH type of neural network. *International Journal of Heat and Mass Transfer* 131:432–41. doi:10.1016/j.ijheatmasstransfer.2018.11.069
- Stritih, U., and V. Butala. 2007. Energy saving in building with PCM cold storage. *International Journal of Energy Research* 31 (15): 1532–44. doi:10.1002/er.1318

- TRNSYS. 2019. Version 18 Thermal energy system specialists. Available from: <http://www.trnsys.com/>.
- Williams, D., L. Elghali, R. Wheeler, and C. France. 2012. Climate change influence on building lifecycle greenhouse gas emissions: Case study of a UK mixed-use development. *Energy and Buildings* 48:112–26. doi:10.1016/j.enbuild.2012.01.016
- Xu, D., S. Boncoeur, G. Tan, J. Xu, H. Qian, and D. Zhao. 2022. *Energy saving potential of a fresh air pre-cooling system using radiative sky cooling*. *Building Simulation* 15 (2):167–78. doi:10.1007/s12273-021-0802-y
- Yu, N., J. Mandal, A. Overvig, N. N. Shi, and M. Tian. 2019. Systems and methods for radiative cooling and heating. WO2016205717A1, Patent Submitted June 18, 2015. <https://www.osti.gov/servlets/purl/1568745>.
- Zhang, S., and J. Niu. 2012. Cooling performance of nocturnal radiative cooling combined with microencapsulated phase change material (MPCM) slurry storage. *Energy and Buildings* 54: 122–30. doi:10.1016/j.enbuild.2012.07.041
- Zhao, D., A. Aili, Y. Zhai, J. Lu, D. Kidd, G. Tan, X. Yin, and R. Yang. 2019. Subambient cooling of water: Toward real-world applications of daytime radiative cooling. *Joule* 3 (1) :111–23. doi:10.1016/j.joule.2018.10.006
- Zhao, B., M. Hu, X. Ao, N. Chen, and G. Pei. 2019. Radiative cooling: A review of fundamentals, materials, applications, and prospects. *Applied Energy* 236:489–513. doi:10.1016/j.apenergy.2018.12.018
- Zhou, K., N. Miljkovic, and L. Cai. 2021. Performance analysis on system-level integration and operation of daytime radiative cooling technology for air-conditioning in buildings. *Energy and Buildings* 235:110749. doi:10.1016/j.enbuild.2021.110749
- Zinzi, M., and G. Fasano. 2009. Properties and performance of advanced reflective paints to reduce the cooling loads in buildings and mitigate the heat island effect in urban areas. *International Journal of Sustainable Energy* 28 (1-3) :123–39. doi:10.1080/14786450802453314